




Proceeding Paper

Very-Long-Wavelength Infrared Range Type-II Superlattice InAs/InAsSb GaAs/Immersed Photodetectors for High-Operating-Temperature Conditions [†]

Kacper Matuszelański ^{1,2}, Krystian Michalczewski ², Łukasz Kubiszyn ² , Waldemar Gawron ^{1,2} 
and Piotr Martyniuk ^{1,*} 

¹ Applied Physics Institute, Military University of Technology, 2 Kaliskiego St., 00-908 Warsaw, Poland; kacper.matuszelanski@student.wat.edu.pl (K.M.); waldemar.gawron@wat.edu.pl (W.G.)

² VIGO PHOTONICS S.A., 129/133 Poznańska St., 05-850 Ożarów Mazowiecki, Poland; kmichalczewski@vigo.com.pl (K.M.); lkubiszyn@vigo.com.pl (Ł.K.)

* Correspondence: piotr.martyniuk@wat.edu.pl; Tel.: +48-261839215

[†] Presented at the 17th International Workshop on Advanced Infrared Technology and Applications, Venice, Italy, 10–13 September 2023.

Abstract: Recently, there has been significant interest in type-II superlattice (T2SL) infrared detectors based on both InAs/GaSb and InAs/InAsSb material systems, and fully operating devices have been presented in the mid- (MWIR) and long-wavelength (LWIR) infrared ranges. In addition, theoretical simulations and experimental reports show high-performance T2SL devices in the very-long-wavelength infrared range (VLWIR) (cutoff wavelength, $\lambda_c \geq 12 \mu\text{m}$). Devices in this wavelength range are essential for space-based applications. In VLWIR, the existing detectors with satisfactory performance are extrinsic silicon detectors operating under heavy, bulky and short-lifetime multistage cryocoolers. These disadvantages are mainly critical for space applications, and thus, developing a device exhibiting a higher operating temperature (HOT) is of high priority. We report on a photoconductive T2SL InAs/InAsSb detector with $\lambda_c > 18 \mu\text{m}$ (limited by a GaAs substrate) and high-operating-temperature (HOT) conditions ($T = 210\text{--}240 \text{ K}$) grown on thick semi-insulating GaAs substrates by molecular beam epitaxy (MBE).

Keywords: VLWIR; T2SLs; InAs/InAsSb; HOT



Citation: Matuszelański, K.; Michalczewski, K.; Kubiszyn, Ł.; Gawron, W.; Martyniuk, P. Very-Long-Wavelength Infrared Range Type-II Superlattice InAs/InAsSb GaAs/Immersed Photodetectors for High-Operating-Temperature Conditions. *Eng. Proc.* **2023**, *51*, 45. <https://doi.org/10.3390/engproc2023051045>

Academic Editors: Gianluca Cadelano, Giovanni Ferrarini and Davide Moroni

Published: 27 December 2023



Copyright: © 2023 by the authors. Licensee MDPI, Basel, Switzerland. This article is an open access article distributed under the terms and conditions of the Creative Commons Attribution (CC BY) license (<https://creativecommons.org/licenses/by/4.0/>).

1. Introduction

Lately, there has been considerable interest in type-II superlattice (T2SL) infrared detectors based on InAs/GaSb and “Ga-free” InAs/InAsSb material systems, and fully operating devices competing with HgCdTe have been presented in the mid- (MWIR) and long-wavelength (LWIR) infrared ranges [1,2]. In addition, theoretical simulations and experimental reports prove that T2SLs devices show high performance in the very-long-wavelength infrared range (VLWIR) (cutoff wavelength, $\lambda_c \geq 12 \mu\text{m}$) [3–5]. VLWIR systems are essential for space applications such as pollution awareness and astronomy [6]. In VLWIR, the existing detectors with satisfactory uniformity and quantum efficiency (*QE*) are extrinsic silicon detectors operating under heavy, bulky and short-lifetime multistage cryocooler conditions [7,8]. These disadvantages are primarily significant for space applications, and thus, detectors exhibiting higher operating temperatures (HOTs, reached by 2–3-stage thermoelectric (TE) cooling) are in high demand. In comparison to extrinsic silicon devices, T2SL devices are based on interband optical transitions allowing them to operate at much higher temperatures. What is more, theoretical simulations and measured results prove that T2SL InAs/InAsSb detectors exhibit a comparable absorption coefficient to HgCdTe, and hence, the development of detectors with high *QE* is feasible [9]. This is why we report on a photoconductive T2SL InAs/InAsSb detector with a cutoff wavelength

of $\lambda_c > 18 \mu\text{m}$ (limited by GaAs substrate transmission) operating at $T = 210\text{--}240 \text{ K}$, grown on a $1.1 \mu\text{m}$ GaSb buffer and a $0.25 \mu\text{m}$ GaAs smoothing layer on a 1.1 mm thick, semi-insulating GaAs substrate (intended to be converted into an immersion lens), by molecular beam epitaxy (MBE). The VLWIR range was reached by growing T2SL InAs/InAsSb detectors in a period (P) of $\sim 14.2 \text{ nm}$ (InAs: $\sim 10.86 \text{ nm}$ and InAsSb: $\sim 3.33 \text{ nm}$, x_{Sb} : ~ 0.4). A net with an active layer thickness of $\sim 1.42 \mu\text{m}$ was grown. Theoretical simulations suggest that the analyzed T2SLs should reach $\lambda_c \sim 28 \mu\text{m}$ (300 K , E_g : $\sim 0.044 \text{ eV}$).

2. Detector Structure

The T2SL InAs/InAsSb wafer was deposited by a RIBER Compact 21-DZ MBE on $2''$ semi-insulating 1.1 mm GaAs (001) substrates. The IMF GaSb buffer layer ($1.1 \mu\text{m}$) was deposited at $500 \text{ }^\circ\text{C}$ on a thin 250 nm GaAs smoothing layer. A detailed description of the buffer growth and substrate processing procedure was presented by Benyahia et al. [10]. Before T2SL deposition, the GaAs substrate was cooled down to $425 \text{ }^\circ\text{C}$ under Sb flux. The T2SLs growth rate was assumed to be at the level of $\sim 0.52 \mu\text{m/h}$. T2SLa deposition was accompanied by short As or As + Sb soaking fluxes to reduce the composition variation at the interfaces.

The absorber consisted of $100 P$ with a $1.42 \mu\text{m}$ net thickness. The VLWIR ($\lambda_c > 18 \mu\text{m}$) was obtained by growing 10.86 nm InAs and 3.33 nm InAsSb ($x_{\text{Sb}} = 0.4$). Assuming no strain in both InAs and InAsSb, the cutoff wavelength was estimated at the level of $\sim 28 \mu\text{m}$ (300 K). Intentional doping was not used during the growth process. The thickness of both the InAs and InAsSb layers was estimated by continuum elastic theory as presented by Polly et al. [11]. The T2SL VLWIR structure is presented in Figure 1a in detail, while Figure 1b presents the XRRD of $100 P$, with the simulation confirming the assumed growth nominal structural parameters of the T2SL InAs/InAsSb detectors to include thickness and x_{Sb} composition (P : $\sim 14.19 \text{ nm}$, InAs: $\sim 10.86 \text{ nm}$, InAsSb: $\sim 3.33 \text{ nm}$, x_{Sb} : ~ 0.4). The FWHM of the 0th-order peak ($2\Theta\text{-}\omega$) was estimated at the level of $\sim 155 \text{ arcsec}$ for the analyzed VLWIR. The detector was mounted on a TO-8 stage, housed with a ZnSe ($\lambda_c \sim 22 \mu\text{m}$) window.

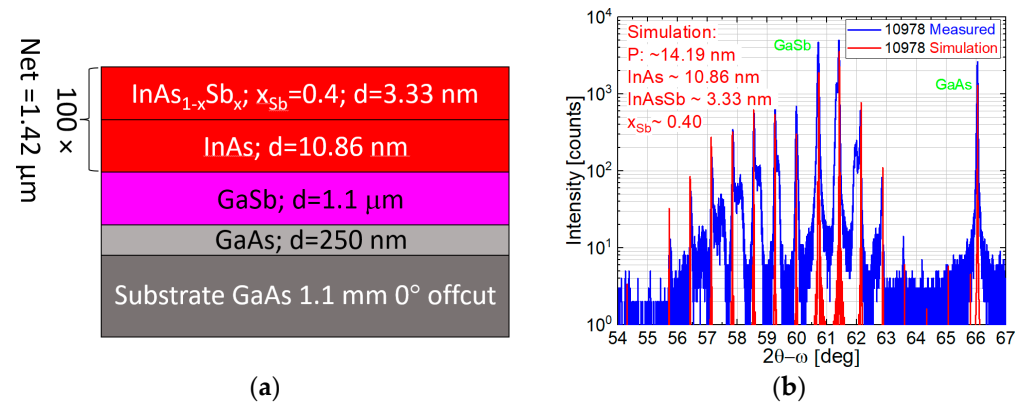


Figure 1. The $\lambda_c > 18 \mu\text{m}$ T2SL InAs/InAsSb (absorber thickness: $1.42 \mu\text{m}$) sample schematic cross section (a) and HRXRD spectrum with T2SL simulation results (b).

3. Results and Discussion

Figure 2 presents the noise for the analyzed detector measured using a low-noise preamplifier and signal analyzer for $V = 0.5 \text{ V}$ and $T = 210\text{--}240 \text{ K}$ ($f = 1\text{--}100 \text{ kHz}$). The noise VLWIR device at 20 kHz ($T = 210\text{--}240 \text{ K}$) stays within $\sim 2.47 \times 10^{-10}\text{--}3.2 \times 10^{-10} \text{ A/Hz}^{1/2}$. The Johnson noise was estimated by the relation $I_j^2 = \frac{4kT}{R_d}$, where R_d is the detector resistance and k is the Boltzmann constant. The Johnson noise of the analyzed VLWIR detector when $T = 210\text{--}240 \text{ K}$ was assessed within the range of $\sim 1.89\text{--}2.34 \times 10^{-11} \text{ A/Hz}^{1/2}$.

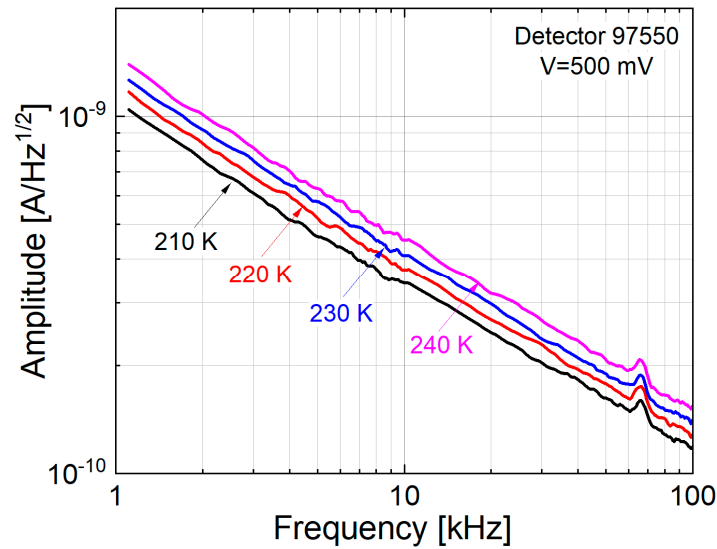


Figure 2. The noise spectra for the analyzed VLWIR single-pixel immersed photoconductor for $V = 0.5$ V and $T = 210$ – 240 K ($f = 1$ – 100 kHz).

The responsivity was measured by FTIR with reference to the calibrated photodetector. The current responsivity versus wavelength is presented in Figure 3a, where $R_i = 0.041$ – 0.016 A/W (@ $16 \mu\text{m}$) when $T = 210$ – 240 K. The device resistance was measured within the range of 31 – 23.1Ω .

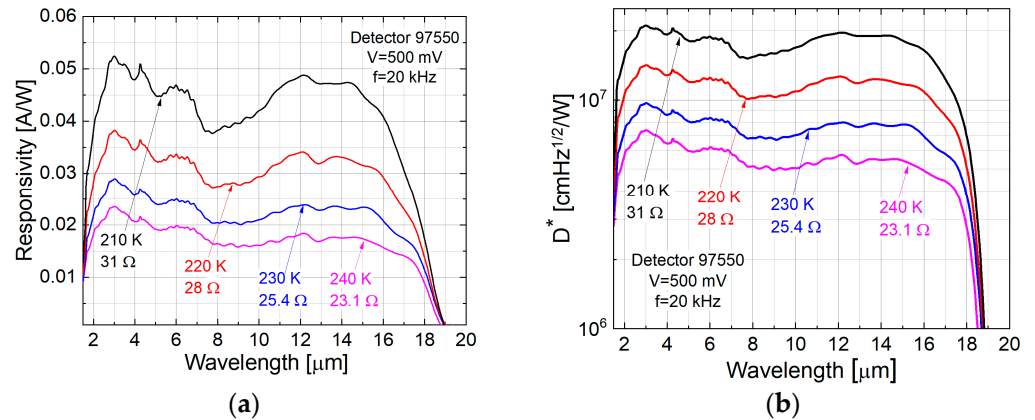


Figure 3. T2SLs InAs/InAsSb VLWIR device’s R_i (a) and D^* (b) for $V = 0.5$ V and $T = 210$ – 240 K.

The specific detectivity was assessed by the equation $D^* = R_i / \sqrt{I_n^2 / A_o \Delta f}$, where R_i is the measured responsivity, A_o is the optical area and I_n is the net noise current. Detectivity versus wavelength is shown in Figure 3b, where $D^* = 1.7 \times 10^7$ – 4.9×10^6 $\text{cmHz}^{1/2}/\text{W}$ for (@ $16 \mu\text{m}$) is estimated. Razeghi et al. reported on VLWIR T2SL InAs/GaSb-based photodiodes with cutoff wavelengths of $\sim 19 \mu\text{m}$ and $\sim 32 \mu\text{m}$ exhibiting detectivity of $\sim 3.71 \times 10^{10}$ $\text{cmHz}^{1/2}/\text{W}$ at 50 K and $\sim 1.05 \times 10^{10}$ $\text{cmHz}^{1/2}/\text{W}$ at 34 K, respectively [12]. In addition, Table 1 presents a performance comparison between T2SL InAs/InAsSb- and HgCdTe-based 2-, 3- and 4-stage TE immersed photoconductors (PCIs) [13].

Table 1. D^* comparison of the T2SL InAs/InAsSb and HgCdTe PCIs for selected temperatures (195, 210, 230, 300 K) and operating wavelengths (10.6, 13, 14, 16 μm) for 20 kHz.

Detector	Material	T (K)	λ (μm)	D^* ($\text{cmHz}^{1/2}/\text{W}$)	
PCI	T2SLs InAs/InAsSb	210	10.6	$\sim 1.8 \times 10^7$	
			13	$\sim 1.9 \times 10^7$	
			14	$\sim 1.9 \times 10^7$	
			16	$\sim 1.6 \times 10^7$	
		230	10.6	$\sim 7.4 \times 10^6$	
			13	$\sim 7.6 \times 10^6$	
			14	$\sim 7.8 \times 10^6$	
			16	$\sim 6.9 \times 10^6$	
		HgCdTe	195	10.6	$\geq 3.0 \times 10^9$
				13	$\geq 1.0 \times 10^9$
				14	$\geq 3.0 \times 10^8$
			210	10.6	$\geq 2.5 \times 10^9$
	13			$\geq 4.5 \times 10^8$	
	230		10.6	$\geq 1.0 \times 10^9$	
		13	$\geq 2.3 \times 10^8$		
	300	10.6	$\geq 8 \times 10^7$		

4. Conclusions

The VLWIR detectors showed that a proper device architecture and immersion lens allow them to compete with HgCdTe TE cooled detectors. The theoretical simulations suggest that presented device reaches a cutoff wavelength of $\sim 28 \mu\text{m}$ (300 K) with $D^* = 1.7 \times 10^7$ – $4.9 \times 10^6 \text{ cmHz}^{1/2}/\text{W}$ for (@16 μm) when $T = 210$ – 240 K .

Author Contributions: Conceptualization, P.M. and W.G.; methodology, P.M. and K.M. (Krystian Michalczewski); validation, P.M., W.G. and K.M. (Krystian Michalczewski); formal analysis, K.M. (Kacper Matuszelański) and Ł.K.; investigation, K.M. (Kacper Matuszelański) and Ł.K.; resources, K.M. (Kacper Matuszelański); data curation, K.M. (Kacper Matuszelański), Ł.K. and P.M.; writing—original draft preparation, P.M.; writing—review and editing, K.M. (Krystian Michalczewski) and Ł.K.; visualization, P.M.; supervision, P.M.; project administration, P.M.; funding acquisition, P.M. All authors have read and agreed to the published version of the manuscript.

Funding: This research was funded by the National Science Centre grant OPUS UMO-2021/43/B/ST7/00768.

Institutional Review Board Statement: Not applicable.

Informed Consent Statement: Not applicable.

Data Availability Statement: The data that support the funding of this study are available from the corresponding author, P.M., upon request.

Conflicts of Interest: Authors Kacper Matuszelański, Krystian Michalczewski, Łukasz Kubiszyn, Waldemar Gawron are employed by the company VIGO PHOTONICS S.A. The remaining author declare that the research was conducted in the absence of any commercial or financial relationships that could be construed as a potential conflict of interest.

References

1. Rogalski, A.; Martyniuk, P.; Kopytko, M. Type-II superlattice photodetectors versus HgCdTe photodiodes. *Prog. Quantum Electron.* **2019**, *68*, 100228. [[CrossRef](#)]
2. Li, Q.; Xie, R.; Wang, F.; Liu, S.; Zhang, K.; Zhang, T.; Gu, Y.; Guo, J.; He, T.; Wang, Y.; et al. SRH suppressed P-G-I design for very long-wavelength infrared HgCdTe photodiodes. *Opt. Express* **2022**, *30*, 16509–16517. [[CrossRef](#)] [[PubMed](#)]
3. Mohseni, H.; Razeghi, M.; Brown, G.J.; Park, Y.S. High-performance InAs/GaSb superlattice photodiodes for the very long wavelength infrared range. *Appl. Phys. Lett.* **2001**, *78*, 2107–2109. [[CrossRef](#)]
4. Mohseni, H.; Tahraoui, A.; Wojkowski, J.; Razeghi, M.; Brown, G.J.; Mitchel, W.C.; Park, Y.S. Very long wavelength infrared type-II detectors operating at 80 K. *Appl. Phys. Lett.* **2000**, *77*, 1572–1574. [[CrossRef](#)]
5. Michalczewski, K.; Martyniuk, P.; Łukasz, K.; Wu, C.H.; Wu, Y.R.; Jureńczyk, J.; Rogalski, A.; Piótrowski, J. Demonstration of the Very Long Wavelength Infrared Type-II Superlattice InAs/InAsSb GaAs Immersed Photodetector Operating at Thermoelectric Cooling. *IEEE Electron Device Lett.* **2019**, *40*, 1396–1398. [[CrossRef](#)]
6. Abedin, M.N.; Martin, G.M.; Tamer, F.R. Infrared detectors overview in the short-wave infrared to far-infrared for CLARREO mission. *Proc. SPIE* **2010**, *7808*, 78080V. [[CrossRef](#)]
7. Deng, K.; Zhang, K.; Li, Q.; He, T.; Xiao, Y.; Guo, J.; Zhang, T.; Zhu, H.; Wang, P.; Li, N.; et al. High-operating temperature far-infrared Si:Ga blocked-impurity-band detectors. *Appl. Phys. Lett.* **2022**, *120*, 211103. [[CrossRef](#)]
8. Beeman, J.W.; Goyal, S.; Reichertz, L.A.; Haller, E.E. Ion-implanted Ge:B far-infrared blocked-impurity-band detectors. *Infrared Phys. Technol.* **2007**, *51*, 60–65. [[CrossRef](#)]
9. Rogalski, A.; Martyniuk, P.; Kopytko, M.; Madejczyk, P.; Krishna, S. InAsSb-Based Infrared Photodetectors: Thirty Years Later On. *Sensors* **2020**, *20*, 7047. [[CrossRef](#)] [[PubMed](#)]
10. Benyahia, D.; Kubiszyn, Ł.; Michalczewski, K.; Kębłowski, A.; Martyniuk, P.; Piotrowski, J.; Rogalski, A. Optimization of the interfacial misfit array growth mode of GaSb epilayers on GaAs substrate. *J. Cryst. Growth* **2018**, *483*, 26–30. [[CrossRef](#)]
11. Polly, S.J.; Bailey, C.G.; Grede, A.J.; Forbes, D.V.; Hubbard, S.M. Calculation of strain compensation thickness for III–V semiconductor quantum dot superlattices. *J. Cryst. Growth* **2016**, *454*, 64–70. [[CrossRef](#)]
12. Razeghi, M.; Wei, Y.; Gin, A.; Hood, A.; Yazdanpanah, V.; Tidrow, M.; Nathan, V. High performance Type II InAs/GaSb superlattices for mid, long, and very long wavelength infrared focal plane arrays. *Proc. SPIE—Int. Soc. Opt. Eng.* **2005**, *5783*, 86–97. [[CrossRef](#)]
13. VIGO Photonics. Available online: <https://vigo.com.pl/wp-content/uploads/2017/06/VIGO-Catalogue.pdf> (accessed on 1 September 2020).

Disclaimer/Publisher’s Note: The statements, opinions and data contained in all publications are solely those of the individual author(s) and contributor(s) and not of MDPI and/or the editor(s). MDPI and/or the editor(s) disclaim responsibility for any injury to people or property resulting from any ideas, methods, instructions or products referred to in the content.